Multi-rate coprime sampling for frequency estimation with increased degrees of freedom

Zhe Fu, Pascal Chargé, Yide Wang

Version of Record: https://www.sciencedirect.com/science/article/pii/S016516841930310X
Manuscript_08affd283b2f25e4f1c2cf97ca1e9947

Multi-rate coprime sampling for frequency estimation with increased degrees of freedom

Zhe Fu, Pascal Chargé, Yide Wang

Institut d'Électronique et de Télécommunications de Rennes (IETR), UMR CNRS 6164, Université de Nantes, Rue Christian Pauc BP 50609, Nantes 44306, France

Abstract

For frequency estimation, the recently proposed coprime sampling scheme receives increasing interest as it reduces sampling rate and exhibits high degrees of freedom. However, the virtual coarray generated by coprime configuration is a linear virtual array structure with some missing elements. This leads to information loss if only the contiguous part of the virtual coarray is used. In this paper, we propose a new approach to fix this problem. A multi-rate coprime sampling mechanism is designed to fill all the holes in the classical coprime virtual coarray. This is achieved by constructing new virtual coarrays containing the hole elements which can be selected to fill all the holes in the original virtual coarray. Furthermore, by properly setting the multi-rate coefficients to positive integers, our approach allows to reuse some samples obtained with the classical coprime sampling configuration. The closed-form expression of the positions of the holes is also given, which can be used to choose the appropriate multi-rate coefficients. Simulation results show that the proposed approach can increase the degrees of freedom without requiring additional samples. The estimation accuracy is also improved because our proposed approach fully exploits the information from the available samples.

Keywords:

Coprime sampling, multi-rate, frequency estimation, virtual coarray interpolation.

1. Introduction

Recently, along with the increasing wireless applications, spectrum shortage has become a bottleneck to wireless communication industry [1, 2]. To ease the overcrowded frequency spectrum, a promising strategy is cognitive radio [3, 4, 5], which efficiently exploits the available spectrum opportunities by allowing the second users to use the licensed frequency bands. To that end, the licensed frequency bands over a wide spectrum need to be sensed in order to detect the unoccupied bands. Many techniques have been developed to dynamically detect frequency bands, including energy detection, match filtering, and cyclostationary feature

detection [6, 7, 8], etc. Due to the well known Shannon-Nyquist theorem, most of the above mentioned techniques are limited by the Nyquist sampling rate. This could result in high implementation complexity to hardware when the bandwidth is large [9, 10, 11].

To lighten the sampling burden on hardware implementation, many sub-Nyquist sampling techniques have been proposed [12, 13, 14, 15, 16, 17]. Among them, some techniques reduce the sampling burden by utilizing the concept of difference coarray [18]. The difference coarray exploits the collected samples to generate a virtual data set, which is equivalent to a virtual sampler working under Nyquist sampling rate. By doing so, the virtual Nyquist rate samples can be constructed by using some sparse samples. We refer to this virtual sampler as virtual difference coarray in this paper. The resultant difference coarray allows increasing greatly the degrees of freedom (DOF) with few sparse samples.

The nested sampling configuration [19, 20] and the minimum redundancy sampling [21, 22] can also increase the DOF. However, the nested sampling, which yields a contiguous coarray structure, consists of two different parts of samples. One part includes some sparse samples with large sampling interval. But the other part is composed of some dense samples obtained with Nyquist rate, which could still cause high hardware complexity. The minimum redundancy sampling can avoid to sample at the Nyquist rate but the samplers do not have a closed-form expression. Combinatorial search is needed before determining the sampling strategy.

The recently proposed coprime sampling mechanism [23, 24, 25] has been considered as an attractive strategy because the sampling rate can be significantly reduced and closed-form coprime sampling strategy can be easily implemented with two conventional samplers. Qin *et al.* [26] further increase the DOF by dividing the samples into units. Several units are simultaneously utilized to form a larger sample block in order to increase the aperture of virtual difference coarray. However, there are some missing elements in the coprime difference coarray, which are considered as holes. It is difficult to directly use the non-continuous virtual coarray for frequency estimation. A common countermeasure is to use only the maximum contiguous part in the difference coarray and discard the discontinuous part. Unfortunately it leads to the loss of DOF because some information in the virtual coarray is not used.

Many interpolation techniques have been proposed for coprime array in direction of arrivals (DOA) finding domain to construct a complete virtual coarray and handle the DOF loss problem. A nuclear norm minimization based interpolation algorithm [27] has been proposed to interpolate the holes. However, the interpolation performance could be affected by finite number of snapshots. As the virtual coarray is a uniform linear array-like structure, the Toeplitz property of covariance matrix can be utilized for interpolating the

missing elements [28, 29, 30]. Zhou *et al.* [31] first divide the virtual coarray signals into multiple virtual measurements, considered as atoms, then the atomic norm minimization technique is applied to reconstruct the Toeplitz covariance matrix. Another high resolution algorithm is to exploit multiple frequencies [32, 33] to generate multiple scaled versions of virtual coarrays for interpolation. This could have a high implementation cost because some physical sensors are required to collect sample snapshots at different frequencies. It is worth noting that this technique, which is proposed for DOA estimation, can not be directly used for frequency estimation without adaptation.

In this paper, inspired by the technique proposed in [32] and [33] which is designed for DOA estimation by a coprime array, we propose a novel interpolation mechanism which is specific to coprime sampling based frequency estimation. We design a multi-rate coprime sampling mechanism to fill the missing elements in the virtual coarray. Multi-rate coefficients are introduced to construct the scaled versions of the virtual coarray. By properly selecting a set of multi-rate coefficients based on the positions of the holes, all the missing elements can be recovered from the scaled virtual coarrays and the holes can be filled. After retrieving the whole uniform linear structure of the virtual coarray, all the coprime sampling samples can be exploited for frequency estimation. The main contributions of this paper are summarized as follows:

1) A novel multi-rate coprime sampling mechanism is designed to fill all the holes in the classical coprime virtual coarray such that the total available DOF provided by coprime sampling can be exploited. We show that no additional hardware implementation is required for the interpolation if the multi-rate coefficients are chosen as some appropriate positive integer values related to the positions of the holes. The complete uniform virtual coarray structure can be retrieved from the original sample stream obtained from the classical coprime sampling scheme, and no additional samples are required. This proposed method is of great importance since the coprime sampling sample stream can be used more effectively. Moreover, the proposed method can also be easily extended to the generalized coprime sampling scheme, which can further increase the DOF.

2) The closed-form expression of all positions of the holes is derived. Though similar expression has been reported in [26, 34], only the lower bound of the holes (first hole) has been explicitly given. The upper bound of positions of the holes has not yet been reported and the holes close to position $(2M-1)N$ can only be obtained by combinatorial search. We derive both the lower bound and upper bound in this paper such that all the positions of the holes can be analytically obtained.

The rest of this paper is organized as follows. The classical coprime sampling model is reviewed in Section 2. The proposed multi-rate coprime sampling scheme and the positions of the holes are described in Section 3. Section 4 provides some simulation results and the conclusion is drawn in Section 5.

2. Signal Model

Consider a signal composed of D sinusoidal components buried in noise

$$x(t) = \sum_{i=1}^{D} A_i e^{j(2\pi f_i t + \phi_i)} + \omega(t) \tag{1}$$

where A_i is the amplitude, f_i the frequency of the i-th sinusoidal component, ϕ_i the corresponding phase assumed to be uniformly distributed in $[0, 2\pi]$ and uncorrelated to each other, and $\omega(t)$ is zero mean additive white Gaussian noise.

As proposed in [24] and [26], two sub-Nyquist samplers operating at sampling intervals MT and NT respectively are utilized to sample the noise contaminated signal, with M and N two coprime integers and $\frac{1}{T} = 2f_{max}$ the Nyquist rate ($f_{max} > max(f_1, f_2, ..., f_D)$). The output samples of the two samplers are denoted by $x_M[n] = x(MnT)$ and $x_N[m] = x(NmT)$, where n and m are non-negative integers. Figure 1 shows the sampling time indices of the two samplers where the values of Mn for the sampler x_M and Nm for the sampler x_N are given by integers below the triangles of the first row and second row respectively.

The k-th sample unit collected at the output of the sampler x_M is a collection of N samples in the time interval $[(k-1)MNT, kMNT)$, for any given positive integer k. Likewise, the corresponding sample unit collected at the output of the sampler x_N is a collection of M samples in the time interval $[(k-1)MNT, kMNT)$. Without loss of generality, a sampling block is defined [24] as the collection of a sample unit, whose first sample index is $(k-1)MN$ for the sampler output x_M and two successive sample units with the same first sample index $(k-1)MN$ for the sampler output x_N, i.e. the red rectangle and blue rectangle in Figure 1 represent two different blocks. In this paper, we refer to this scheme as the classical coprime sampling. Two sample subsets associated with the l-th ($l \geq 0$) block can be expressed as

$$x_M[Nl+n] = \sum_{i=1}^{D} A_i e^{j\left(\pi q_i M(Nl+n)+\phi_i\right)} + \omega(M(Nl+n)T) \tag{2}$$

$$x_N[Ml+m] = \sum_{i=1}^{D} A_i e^{j\left(\pi q_i N(Ml+m)+\phi_i\right)} + \omega(N(Ml+m)T) \tag{3}$$

where $q_i = 2f_iT = \frac{f_i}{f_{max}}$ is the normalized frequency with $q_i \in (-1, 1)$, and m, n are the indices of samples in the l-th block with $1 \leq m \leq 2M-1, 0 \leq n \leq N-1$.

The following sampling signal vectors of the two samplers can be constructed with the above samples

$$\mathbf{y}_M[l] = [x_M[Nl], x_M[Nl+1], ..., x_M[Nl+N-1]]^T \tag{4}$$

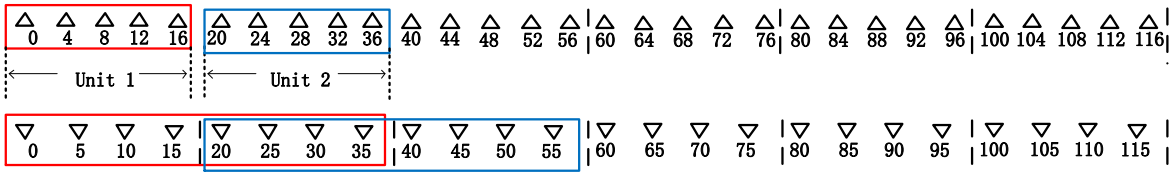

Figure 1: Sampling time indices set of two samplers, $M = 4$ and $N = 5$.

$$\mathbf{y}_N[l] \quad = \quad [x_N[Ml+1], ..., x_N[Ml+2M-1]]^T \tag{5}$$

Concatenating $\mathbf{y}_M[l]$ and $\mathbf{y}_N[l]$, the whole sampling signal vector of the l-th block can be constructed as

$$\begin{aligned} \mathbf{y}[l] &= [\mathbf{y}_M^T[l], \mathbf{y}_N^T[l]]^T = \sum_{i=1}^{D} \mathbf{a}(q_i) A_i e^{j\phi_i} e^{j\pi q_i MNl} + \mathbf{n}[l] \\ &= \mathbf{A}_s \mathbf{s}(l) + \mathbf{n}[l] \end{aligned} \tag{6}$$

where $\mathbf{A}_s = [\mathbf{a}(q_1), \mathbf{a}(q_2), ..., \mathbf{a}(q_D)]$, $\mathbf{s}(l) = [A_1 e^{j(q_1\pi MNl+\phi_1)}, A_2 e^{j(q_2\pi MNl+\phi_2)}, ... \ A_D e^{j(q_D\pi MNl+\phi_D)}]^T$, $\mathbf{a}(q_i) = [[1 ... e^{jq_i\pi M(N-1)}] \quad [e^{jq_i\pi N} ... \quad e^{jq_i\pi N(2M-1)}]]^T$, and $\mathbf{n}[l]$ is the corresponding noise vector. From the hypothesis on the received signal, the covariance matrix of $\mathbf{y}[l]$ can be written as

$$\begin{aligned} \mathbf{R}_\mathbf{y} &= E[\mathbf{y}[l]\mathbf{y}^H[l]] = \mathbf{A}_s \mathbf{R}_s \mathbf{A}_s^H + \sigma_n^2 \mathbf{I} \\ &= \sum_{i=1}^{D} A_i^2 \mathbf{a}(q_i)\mathbf{a}^H(q_i) + \sigma_n^2 \mathbf{I} \end{aligned} \tag{7}$$

where $\mathbf{R}_s = diag[p_1, p_2, ..., p_D]$ with $p_i = A_i^2, i = 1, 2, ..., D$, σ_n^2 is the noise power and $\mathbf{I}$ is a $(N + 2M - 1) \times (N + 2M - 1)$ identity matrix. Matrix $\mathbf{R}_\mathbf{y}$ contains both the self-lags and cross-lags correlation of the two sample streams. The self-lags and cross-lags can be represented by the following difference coarray integers set

$$\mathbb{L} = \{\pm(Mn - Nm)\} \tag{8}$$

The maximum value in $\mathbb{L}$ is $(2M - 1)N$, which is much larger than $2M + N - 1$ for two coprime integers. Coprime sampling scheme uses the concept of difference coarray to construct a virtual coarray and increase the DOF. Elements in $\mathbb{L}$ can be equivalently considered as the indices of a virtual Nyquist rate sampler, whose samples are the corresponding elements in $\mathbf{R}_\mathbf{y}$.

The equivalent virtual signal can be obtained by reshaping the covariance matrix $\mathbf{R_y}$ as follows

$$\mathbf{r} = vec(\mathbf{R_y}) = \sum_{i=1}^{D} p_i \mathbf{a}^*(q_i) \otimes \mathbf{a}(q_i) + \sigma_n^2 \mathbf{i} = \mathbf{A}_c \mathbf{p} + \sigma_n^2 \mathbf{i} \tag{9}$$

where $\mathbf{A}_c = \mathbf{A}_s^* \odot \mathbf{A}_s$, $\mathbf{p} = [p_1, p_2, ..., p_D]^T$, $\odot$ denotes the Khatri-Rao product, $\otimes$ denotes the Kronecker product and $\mathbf{i} = vec(\mathbf{I})$.

3. Multi-rate coprime sampling

It can be noticed that the vectorized vector $\mathbf{r}$ contains all the self-lags and cross-lags correlation. By selecting the appropriate elements corresponding to the self-lags and cross-lags in $\mathbb{L}$ (8), we can construct the virtual coarray integer set ranging from $-(2M-1)N$ to $(2M-1)N$ [35], in which some missing elements exist. An illustration of the virtual coarray is given in Figure 2a with $M = 4, N = 5$. It is clear that there are some holes in the virtual coarray and the nonuniform coarray can not be directly employed for efficient frequency estimation. In this section, we elaborate how the holes can be filled by exploiting multi-rate coprime sampling without additional samples, such that all the information included in the virtual coarray can be fully exploited.

It is worth noting that we consider the classical coprime sampling [24] to elaborate the proposed method in this paper. The proposed multi-rate method can be easily extended to the generalized coprime sampling scheme [26] by choosing appropriate sampling rate in accordance with the positions of the holes. By doing so, the DOF can be further increased.

3.1. Multiple rate coprime sampling

Consider two samplers similar to Figure 1, whose sampling intervals are $a_r MT$ and $a_r NT$ with a_r the multi-rate coefficient ($a_r > 0$), respectively, the two collected sample subsets associated with the l-th block are given by

$$\begin{aligned} x_{M,a_r}[Nl+n] &= \sum_{i=1}^{D} A_i e^{j\left(\pi q_i a_r M(Nl+n)+\phi_i\right)} + \omega(a_r M(Nl+n)T) \\ x_{N,a_r}[Ml+m] &= \sum_{i=1}^{D} A_i e^{j\left(\pi q_i a_r N(Ml+m)+\phi_i\right)} + \omega(a_r N(Ml+m)T) \end{aligned}$$

where $x_{M,a_r}[Nl+n] = x(M(Nl+n)a_r T)$, $x_{N,a_r}[Ml+m] = x(N(Ml+m)a_r T)$, with $1 \le m \le 2M-1$, $0 \le n \le N-1$. It can be observed that the number of elements in each block remains the same as in the

original classical coprime sampling, while the sampling interval is scaled up by a factor a_r. The corresponding sampling signal vector of the l-th block can be written as

$$\mathbf{y}_{a_r}[l] = \sum_{i=1}^{D} \mathbf{a}(a_r q_i) A_i e^{j\phi_i} e^{j\pi q_i a_r MNl} + \mathbf{n}_{a_r}[l] \tag{10}$$

its covariance matrix can be expressed as

$$\mathbf{R}_{\mathbf{y}}(a_r) = E[\mathbf{y}_{a_r}[l]\mathbf{y}_{a_r}^H[l]] = \sum_{i=1}^{D} A_i^2 \mathbf{a}(a_r q_i)\mathbf{a}^H(a_r q_i) + \sigma_n^2 \mathbf{I} \tag{11}$$

Similarly to (8), the self-lags and cross-lags under sampling rates $a_r MT$ and $a_r NT$ can be described by the following set

$$\mathbb{L}(a_r) = \{\pm a_r(Mn - Nm)\} \tag{12}$$

It is obvious that $\mathbb{L}(a_r)$ is a scaled version of $\mathbb{L}$ with multi-rate coefficient a_r. With an appropriate value of a_r, $\mathbb{L}(a_r)$ can include some missing elements in $\mathbb{L}$. After vectorizing and rearranging the elements, the virtual coarray obtained with sampling rates $a_r MT$ and $a_r NT$ contains some hole elements that occur in the virtual coarray of sampling rates MT and NT. The idea of multi-rate coprime scheme is to find all the hole elements from the resultant virtual coarrays generated by multi-rate coprime sampling. These elements can be employed to fill the holes in the classical coprime coarray. This is achieved by choosing some appropriate values of a_r in accordance with the positions of the holes.

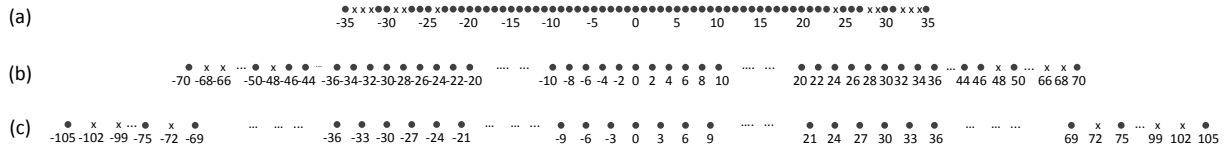

Figure 2: Sampling indices of virtual coarrays with different sampling rates. (a) Sampling rates MT, NT (b) Sampling rates $2MT, 2NT$ (c) Sampling rates $3MT, 3NT$, with $M = 4$ and $N = 5$, •: existed elements, ×: holes.

3.2. Virtual covariance matrix construction

The maximum value in $\mathbb{L}$ is $K = (2M - 1)N$. We consider a covariance matrix $\mathbf{R}_v$ that can utilize all the DOF. Therefore, we can define a set of values corresponding to the full DOF as

$$\mathbb{L}_{DOF} = \{\pm i | 0 \leq i \leq K\} \tag{13}$$

Then we can construct the following Toeplitz covariance matrix

$$\mathbf{R}_v = \begin{pmatrix} r[0] & r[-1] & ... & r[-K] \\ r[1] & r[0] & ... & r[-K+1] \\ ... & ... & ... & ... \\ r[K] & r[K-1] & ... & r[0] \end{pmatrix} \tag{14}$$

where $r[i] = E[x(t)x^*(t-iT)]$ only depends on the lag $i = 0, 1, ..., (2M-1)N$. In other words, $r[i]$ corresponds to the data of the i-th position in the virtual coarray. An example of virtual coarray with $M = 4, N = 5$ is shown in Figure 2a. For a given realization, $\mathbf{R}_v$ and $r[i]$ are represented by $\hat{\mathbf{R}}_v$ and $\hat{r}[i]$.

To estimate $r[i]$, the covariance matrix (7) is estimated by averaging the available sample blocks

$$\hat{\mathbf{R}}_{\mathbf{y}} = \frac{1}{L}\sum_{l=0}^{L-1} \mathbf{y}[l]\mathbf{y}^H[l] \tag{15}$$

where L is the number of blocks. For the i-th position in the virtual coarray, there may be several elements in $\hat{\mathbf{R}}_{\mathbf{y}}$ that correspond to the same position. The i-th position $r[i]$ is estimated by averaging all the corresponding elements in $\hat{\mathbf{R}}_{\mathbf{y}}$ and the respective element $\hat{r}[i]$ is obtained [33].

Notice that there are some missing integers in $\mathbb{L}$ which are related to the missing elements in $\hat{\mathbf{R}}_v$. These elements correspond to the holes that can not be directly obtained from $\hat{\mathbf{R}}_{\mathbf{y}}$. We define the missing elements set as

$$\mathbb{L}_{holes} = \{i | i \in (\mathbb{L}_{DOF} - \mathbb{L})\} \tag{16}$$

Alternatively, a new covariance matrix can be estimated under multi-rate coprime sampling with coefficient a_r, which is represented by $\hat{\mathbf{R}}_{\mathbf{y}}(a_r)$. By choosing some appropriate values of a_r, the set of lags associated with $\hat{\mathbf{R}}_{\mathbf{y}}(a_r)$ can be equivalently represented as (12). All the missing elements $\hat{r}[i]$ can be obtained from the intersection between $\mathbb{L}_{holes}$ and the selected sets $\mathbb{L}(a_r)$ to retrieve matrix $\hat{\mathbf{R}}_v$. In other words, we can define $\mathbb{I}_{rates}$ as a set of selected multi-rate coefficients allowing to fill all the holes such that

$$\mathbb{L}_{holes} = \bigcup_{a_r \in \mathbb{I}_{rates}} \{\mathbb{L}_{holes} \cap \mathbb{L}(a_r)\} \tag{17}$$

For illustration, we consider the holes ± 24 as shown in Figure 2a. Many values of a_r can be used to fill these two holes. A condensed coarray can be obtained with value $a_r = \frac{24}{25}$, which requires to implement another two samplers at new sampling rates $\frac{24}{25}MT$ and $\frac{24}{25}NT$. If we choose $a_r > 1$, the coarray will be extended,

as shown in Figure 2b for $a_r = 2$.

Meanwhile, an interesting fact is that if the multi-rate coefficient a_r is set to be an integer greater than 1, the resultant samples are included in the samples obtained with the initial classical sampling rates MT and NT. These samples can be equivalently considered as the samples of the multi-rate sampling. In other words, these samples can be directly obtained by decimating the original classical coprime samples. A graphic illustration is given in Figure 3 with $M = 4, N = 5$ and $a_r = 2$. This is of great importance to the sampling process because the multi-rate samples can be obtained by choosing the appropriate samples from the classical coprime sampling sample stream. In this case, the resultant multi-rate covariance matrix can be respectively expressed as follows

$$\hat{\mathbf{R}}_{\mathbf{y}}(a_r) = \frac{1}{\lfloor \frac{L}{a_r} \rfloor} \sum_{l=0}^{\lfloor \frac{L}{a_r} \rfloor} \mathbf{y}_{a_r}[l] \mathbf{y}_{a_r}^H[l] \tag{18}$$

Here, only $\frac{1}{a_r}$ samples from the x_M and x_N samplers are chosen for the multi-rate scheme, which indicates that the multi-rate scheme has totally $\lfloor \frac{L}{a_r} \rfloor$ blocks ($\lfloor \cdot \rfloor$ is the floor operator). No additional sampling operation is required and this will not cause extra sampling burden to the samplers. In the following sections, we only consider the case where a_r is an integer greater than 1.

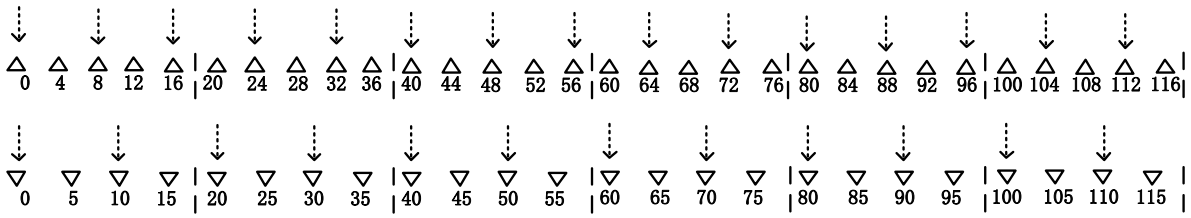

Figure 3: Multi-rate coprime sampling indices selected from the classical coprime sampling, $M = 4, N = 5, a_r = 2$ ↓: sampling indices selected for multi-rate coprime sampling.

Filling holes without data reusing

As shown in Figure 2, we consider $M = 4, N = 5$ to illustrate the mechanism without reusing data. The holes occur at positions $\{\pm 24, \pm 28, \pm 29, \pm 32, \pm 33, \pm 34\}$. As shown in Figure 2b, a new virtual coarray can be constructed by setting $a_r = 2$. It can be easily observed that the lags $\{\pm 24, \pm 28, \pm 32, \pm 34\}$ can be obtained via this new coarray and we can directly select these elements from Figure 2b to fill the holes in Figure 2a. In addition, the holes $\{\pm 33\}$ and $\{\pm 29\}$ can also be filled by setting $a_r = 3$ (Figure 2c) and

$a_r = 29$ respectively. The resultant integer sets can be expressed as

$$\mathbb{L}(a_r = 2) = \{\pm 2(Mn - Nm)\} \tag{19}$$

$$\mathbb{L}(a_r = 3) = \{\pm 3(Mn - Nm)\} \tag{20}$$

$$\mathbb{L}(a_r = 29) = \{\pm 29(Mn - Nm)\} \tag{21}$$

Here, m, n are the indices of samples in one block. By selecting the appropriate elements from $\hat{\mathbf{R}}_{\mathbf{y}}(a_r = 2), \hat{\mathbf{R}}_{\mathbf{y}}(a_r = 3), \hat{\mathbf{R}}_{\mathbf{y}}(a_r = 29)$, the holes in Figure 2a can all be filled correspondingly. It comes that

$$\{\pm 24, \pm 28, \pm 32, \pm 34\} \subseteq \{\mathbb{L}_{holes} \cap \mathbb{L}(a_r = 2)\} \tag{22}$$

$$\{\pm 33\} \subseteq \{\mathbb{L}_{holes} \cap \mathbb{L}(a_r = 3)\} \tag{23}$$

$$\{\pm 29\} \subseteq \{\mathbb{L}_{holes} \cap \mathbb{L}(a_r = 29)\} \tag{24}$$

Notice that each value of a_r can only fill one or several specific holes. In other words, we use only the corresponding elements in each $\hat{\mathbf{R}}_{\mathbf{y}}(a_r)$ to fill the holes and discard the remaining elements. We define this mechanism as data no-reusing mechanism. In the following section, we will explain the data reusing mechanism

Filling holes with data reusing

The estimation variance can generally be reduced if higher number of data can be used for calculating the average value. Comparing Figure 2a, Figure 2b and Figure 2c, it can be found that there are some overlapped positions, i.e., $\{0, \pm 2, \pm 4, \pm 6...\}$ in Figure 2a and Figure 2b, $\{\pm 6, \pm 12, \pm 18...\}$ in Figure 2a, Figure 2b and Figure 2c. It means that $\mathbb{L} \cap \mathbb{L}(a_r)$ is not an empty set. The data in the initial coarray (Figure 2a) are constructed by averaging the respective data from the sampling covariance matrix. In Figure 2b and Figure 2c, though the data from the selected matrices $\hat{\mathbf{R}}_{\mathbf{y}}(a_r)$ are intended to fill the holes, they simultaneously generate some data which can be reused for calculating the overlapped positions in Figure 2a. In this case, we can jointly use all the useful data in $\hat{\mathbf{R}}_{\mathbf{y}}(a_r)$ with the data in $\hat{\mathbf{R}}_{\mathbf{y}}$ to construct the complete virtual coarray.

For illustration, we consider the position $\{\pm 6\}$, which can be found in Figure 2a, Figure 2b and Figure 2c. The respective elements in $\hat{\mathbf{R}}_{\mathbf{y}}$, $\hat{\mathbf{R}}_{\mathbf{y}}(a_r = 2)$, $\hat{\mathbf{R}}_{\mathbf{y}}(a_r = 3)$ can be selected to calculate the average and be used to fill the position $\{\pm 6\}$. This data reusing mechanism can be applied to all the overlapped positions including the holes. The information in the virtual coarrays generated by multi-rates can then be maximally

exploited.

Let us denote the set of multi-rate integer coefficients $\mathbb{I}_{rates}$ as in (17), and define the union set of overlapped positions between the classical coprime coarray and multiple rate coarrays as

$$\mathbb{L}_{rates} = \bigcup_{a_r \in \mathbb{I}_{rates}} \{\mathbb{L} \cap \mathbb{L}(a_r)\} \tag{25}$$

Furthermore, assume that there are N_i entries in $\hat{\mathbf{R}}_{\mathbf{y}}$ and N_{i,a_r} entries in $\hat{\mathbf{R}}_{\mathbf{y}}(a_r)$, which are denoted by $\hat{\mathbf{R}}_{\mathbf{y}}^{(i,k)}, k = 1, 2, ..., N_i$ and $\hat{\mathbf{R}}_{\mathbf{y}}^{(i,k)}(a_r), k = 1, 2, ..., N_{i,a_r}$, which correspond to the same i-th position in the coarray, then the data reusing mechanism can be summarized as follows:

1) If $i \in \{\mathbb{L} - \mathbb{L}_{rates}\}$, we select all the corresponding entries from $\hat{\mathbf{R}}_{\mathbf{y}}$ to calculate $\hat{r}[i]$:

$$\hat{r}[i] = \frac{1}{N_i} \sum_{k=1}^{N_i} \hat{\mathbf{R}}_{\mathbf{y}}^{(i,k)} \tag{26}$$

2) If $i \in \mathbb{L}_{holes}$, we first choose several different values of $a_r \in \mathbb{I}_{rates}$ to generate different versions of $\hat{\mathbf{R}}_{\mathbf{y}}(a_r)$, then select all the corresponding entries from different $\hat{\mathbf{R}}_{\mathbf{y}}(a_r)$ to calculate $\hat{r}[i]$:

$$\hat{r}[i] = \frac{1}{\sum_{a_r \in \mathbb{I}_{rate}} N_{i,a_r}} \sum_{a_r \in \mathbb{I}_{rate}} \sum_{k=1}^{N_{i,a_r}} \hat{\mathbf{R}}_{\mathbf{y}}^{(i,k)}(a_r) \tag{27}$$

3) If $i \in \mathbb{L}_{rates}$, we select all the corresponding entries from $\hat{\mathbf{R}}_{\mathbf{y}}$ as well as the different versions of $\hat{\mathbf{R}}_{\mathbf{y}}(a_r)$ to jointly estimate the mean value of $\hat{r}[i]$:

$$\hat{r}[i] = \frac{1}{N_i + \sum_{a_r \in \mathbb{I}_{rate}} N_{i,a_r}} \left(\sum_{k=1}^{N_i} \hat{\mathbf{R}}_{\mathbf{y}}^{(i,k)} + \sum_{a_r \in \mathbb{I}_{rate}} \sum_{k=1}^{N_{i,a_r}} \hat{\mathbf{R}}_{\mathbf{y}}^{(i,k)}(a_r) \right) \tag{28}$$

It can be noticed that for the covariance matrix $\hat{\mathbf{R}}_{\mathbf{y}}(a_r)$, apart from the entries in $\hat{\mathbf{R}}_{\mathbf{y}}(a_r)$ that are used to estimate $\hat{r}[i]$ for the case $i \in \mathbb{L}_{holes}$, some entries in $\hat{\mathbf{R}}_{\mathbf{y}}(a_r)$ can also be reused to estimate the elements $\hat{r}[i]$ for $i \in \mathbb{L}_{rates}$.

After filling all the holes in the classical coprime virtual coarray, the maximum DOF can be fully used without discarding the non-contiguous part. Many mature techniques can be applied on $\hat{\mathbf{R}}_v$, including MUltiple SIgnal Classification (MUSIC) [36] and Estimation of Signal Parameters via Rotational Invariance Techniques (ESPRIT) [37], etc.

3.3. Suggested rules to choose the multi-rate coefficients

For any given situation, it is clear that different sets of multi-rate $\mathbb{I}_{rates}$ can be defined to fill all the holes. Here we suggest two rules to choose $\mathbb{I}_{rates}$:

• Rule 1: **Choose a_r as small as possible**. This can be seen from equation (18) that smaller a_r can achieve higher value of $\frac{L}{a_r}$, leading to more data for calculating $\hat{\mathbf{R}}_{\mathbf{y}}(a_r)$ and achieving better estimation performance.

• Rule 2: **Make the cardinality of $\mathbb{I}_{rates}$ as small as possible**. In the proposed scheme, we should calculate $\hat{\mathbf{R}}_{\mathbf{y}}(a_r)$ for each value of a_r. It is straightforward that more different coefficients will cause higher calculation complexity. Consequently, the cardinality of $\mathbb{I}_{rates}$ should be as small as possible to reduce the calculation complexity.

To find the appropriate value of a_r, the positions of holes are first obtained by the proposition which will be specified in the next subsection. Then the prime factorization is implemented to find the prime factors of the position value of each hole. According to the prime factors of the position values of all holes, we can choose a_r based on the above two rules. The details are given as follows:

If several values of the positions of holes have one common prime factor (CPF), we choose this CPF as one value of a_r to fill the corresponding holes;

If there exist several common prime factors for several holes, we choose the smallest CPF according to rule 1;

If the position of a hole have no CPF with other holes, we choose its minimum prime factor as one value of a_r.

For any integers greater than 1, we can always find at least one prime factor according to the principle of prime factorization. This means that we can always find at least one suitable $a_r \neq 1$ for any hole value.

For the cases of small value of M and N which have few holes in the coarray, it could be easy to perform the prime factorization and find the suitable a_r. As for the cases of large M and N with more holes, saying more than 10 hole elements (10 is an empirical value), we propose the following algorithm to simplify the process of choosing a_r:

1) We first consider $a_{r1} = 2$. This is because 2 is the smallest prime integer and it is the prime factor of all even integers. By doing so, the holes with even position values can be filled.

2) If there are still many unfilled holes (more than 10 different values), we can choose the next prime integer greater than 2, which is $a_{r2} = 3$, and the holes with position values of multiple of 3 are filled. If there are only a few holes remaining unfilled, the prime factorization is then implemented to the unfilled

holes to find their prime factors and choose the suitable a_r.

The reason we choose $a_{r1} = 2$ is that a smaller integer is a common divisor of more integers, i.e., 2 is the divisor of all even integers while 3 is the divisor of one integer among every three contiguous integers. In general, if there are many holes needed to be filled, a_r with a smaller value can fill more holes.

3.4. Positions of the holes

Before choosing an appropriate value of a_r, the position of missing elements in $\mathbb{L}$ should be first determined. For given system parameters M and N, the following proposition holds:

Proposition: The holes occur at position $\pm(b_1M + b_2N)$, where $b_1M + b_2N < (2M-1)N$, b_1, b_2 are integers, $1 \leq b_1 \leq N - 1 - \lfloor \frac{N}{M} \rfloor$ and $M \leq b_2 \leq 2M - 2$.

It should be noticed that the same expression of positions of the holes has been given in [34]. However, only the lower bounds of b_1 and b_2 are provided. The upper bounds of b_1 and b_2 have not been given. In Appendix, we give the proof for the upper bounds of b_1 and b_2 so that all the holes can be analytically determined. We also provide a new way to prove the lower bounds of b_1 and b_2.

3.5. CRB

The Cramér Rao Bound (CRB) offers a lower bound of estimation variance of any unbiased estimator. The CRB has been widely studied for traditional uniform linear array [38, 39] and coprime coarray [35, 40, 41]. In this section, we give the CRB of the classical coprime sampling. For signal model (7), the parameter vector is defined as

$$\boldsymbol{\eta} = [q_1, ..., q_D, p_1, ...p_D, \sigma_n^2]^T \tag{29}$$

The (i,j)-th element of the Fisher information matrix (FIM) can be given as

$$FIM_{i,j} = L\ trace[\frac{\partial \mathbf{R_y}}{\partial \eta_i}\mathbf{R_y}^{-1}\frac{\partial \mathbf{R_y}}{\partial \eta_j}\mathbf{R_y}^{-1}] \tag{30}$$

Following the similar derivations in [35], FIM can be given as

$$\mathbf{FIM} = L\begin{bmatrix} \mathbf{M}_f^H\mathbf{M}_f & \mathbf{M}_f^H\mathbf{M}_s \\ \mathbf{M}_s^H\mathbf{M}_f & \mathbf{M}_s^H\mathbf{M}_s \end{bmatrix} \tag{31}$$

where

$$\mathbf{M}_f = (\mathbf{R}_\mathbf{y}^T \otimes \mathbf{R}_\mathbf{y})^{-1/2}\mathbf{A}_d\mathbf{R}_s \tag{32}$$

$$\mathbf{M}_s \quad = \quad (\mathbf{R}_{\mathbf{y}}^T \otimes \mathbf{R}_{\mathbf{y}})^{-1/2}[\mathbf{A}_c, \mathbf{i}] \tag{33}$$

with $\mathbf{A}_d = \mathbf{A}_{der}^* \odot \mathbf{A}_s + \mathbf{A}_s^* \odot \mathbf{A}_{der}$ and

$$\mathbf{A}_{der} = \left[\frac{\partial \mathbf{a}(q_1)}{\partial q_1}, \frac{\partial \mathbf{a}(q_2)}{\partial q_2}, ..., \frac{\partial \mathbf{a}(q_D)}{\partial q_D}\right] \tag{34}$$

The CRB of the estimated frequencies can be obtained as

$$\mathbf{CRB}_f = \frac{1}{L}(\mathbf{M}_f^H(\mathbf{I} - \mathbf{M}_s(\mathbf{M}_s^H\mathbf{M}_s)^{-1}\mathbf{M}_s^H)\mathbf{M}_f)^{-1} \tag{35}$$

4. Numerical Results

In this section, the MUSIC algorithm is used for estimating the frequencies. The benchmarks of comparison are to assess the maximum number of detectable frequencies and the relative root mean square error (RMSE) of the estimated frequencies, which is defined as

$$RMSE = \sqrt{\frac{1}{DU}\sum_{i=1}^{D}\sum_{u=1}^{U}(\hat{q}_i(u) - q_i)^2} \tag{36}$$

where $\hat{q}_i(u)$ is the estimate of the normalized frequency q_i in the u-th estimation trial, $u = 1, 2, ..., U$.

4.1. MUSIC spectrum and number of detectable frequencies

We first consider the case of $M = 4$ and $N = 5$ to show the MUSIC spectrum of the proposed multi-rate coprime sampling scheme. The SNR is set to be 0dB and the number of sampling units is set to $L = 1000$. Based on the *Proposition* of positions of the holes in Section 3.4, the set of holes can be determined as $\mathbb{L}_{holes} = \{\pm 24, \pm 28, \pm 29, \pm 32, \pm 33, \pm 34\}$. The maximum number of detectable frequencies of the coarray after filling the holes with the proposed multi-rate coprime scheme is $(2M-1)N = 35$. As explained in the previous section, parameter a_r with values in the set $\mathbb{I}_{rates} = \{2, 3, 29\}$ has been used. $\mathbb{I}_{rates} = \{3, 4, 17, 29\}$ could also be chosen but according to the suggested rules in Section 3.3, it is preferable to use $\mathbb{I}_{rates} = \{2, 3, 29\}$ with three different a_r rather than four.

Figure 4 shows the MUSIC spectrum of 35 estimated frequencies which are uniformly distributed over interval $[-0.96, 0.96]$. The vertical dotted lines correspond to the true positions of frequencies. It can be seen that all the frequencies are correctly estimated using the proposed scheme. It should be mentioned that in the classical coprime sampling, only a maximum of 23 frequencies can be estimated due to the holes,

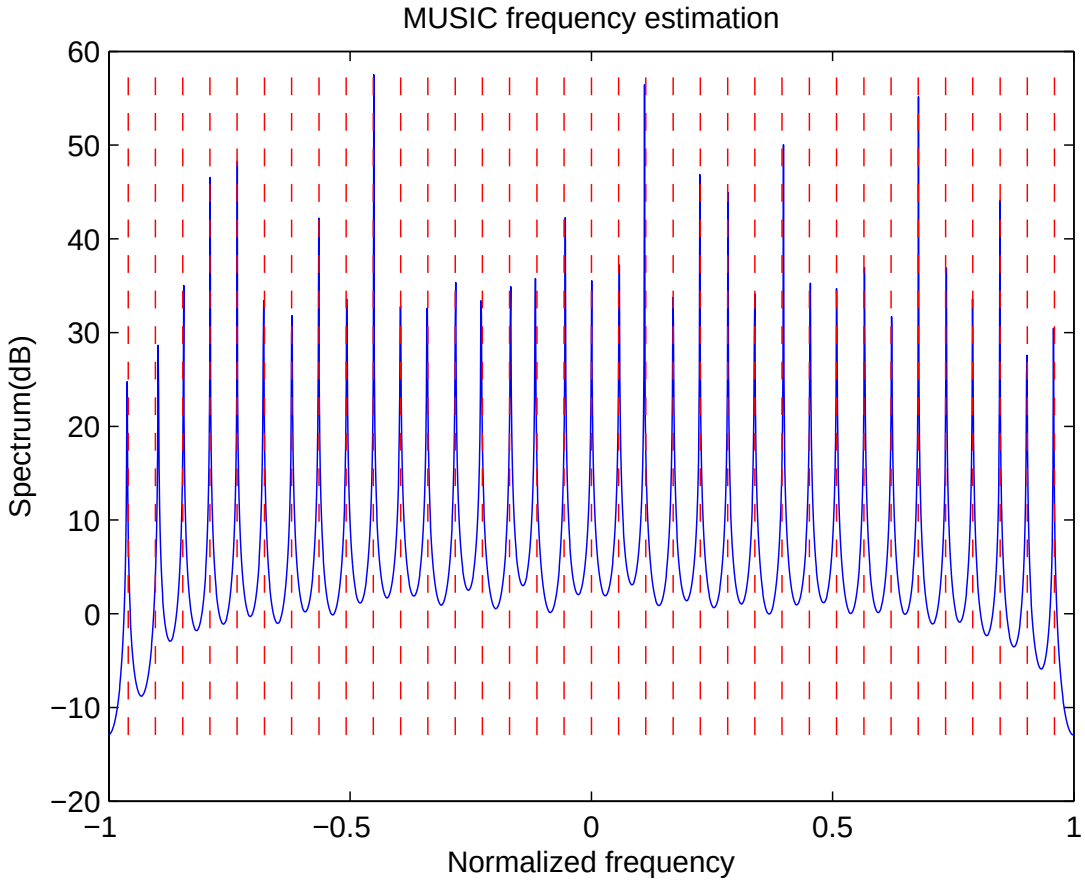

Figure 4: MUSIC spectrum of estimated frequencies, $M = 4, N = 5$, 35 different sinusoidal components.

which means that part of the DOF can not be used. Our proposed scheme can significantly increase the maximum number of detectable frequencies.

4.2. Performance with different multi-rate coefficients

Next, we investigate the impact of the multi-rate coefficient to the proposed scheme. The data no-reusing mechanism is used in Figure 5 to focus on the impact of a_r. For simplicity, we consider a coprime array with $M = 2, N = 3$ which has only one pair of holes in the difference coarray (position ± 8). The number of Monte Carlo trials is set to be 500. We only need to choose one value of a_r to construct a new multi-rate coarray. The possible solutions of integer a_r are $a_r = 2, a_r = 4, a_r = 8$. The classical coprime sampling scheme with no holes filling [24] is compared with these three scenarios.

Figure 5 shows the performance with 4 sinusoidal components. It can be seen that the proposed scheme outperforms the classical coprime sampling scheme. This is mainly because the multiple coprime rate

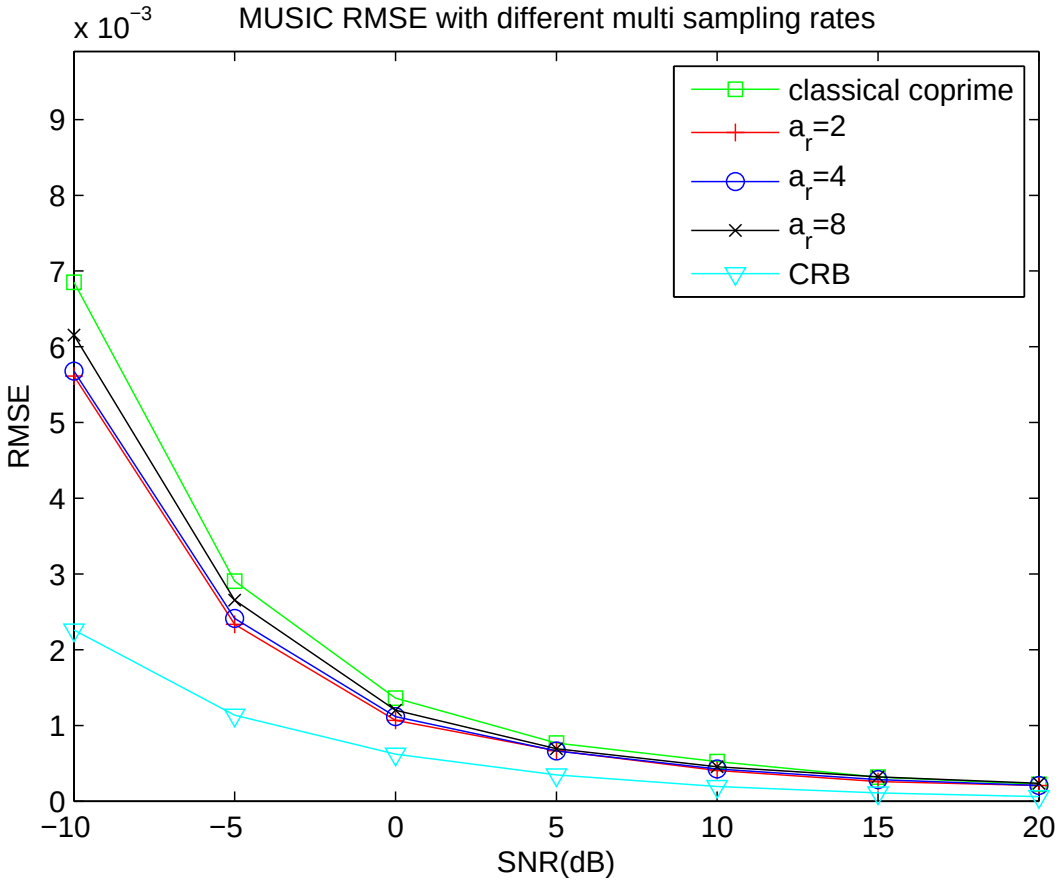

Figure 5: RMSE performance with different multi-rate coefficients, $M = 2, N = 3$, 4 sinusoidal components.

scheme fills the holes in the classical coprime virtual coarray. Therefore, the maximum number of detectable frequencies is 9 for the proposed method, while it is only 7 for the classical coprime scheme with $M = 2, N = 3$.

We can also observe from Figure 5 that a lower value of a_r leads to a better estimation performance. This benefit is due to the fact that more samples are selected from the classical coprime sample stream if a_r is set to a lower value. The estimation variance can be reduced when more samples are used for calculating the average, which is in agreement with the suggested rules in Section 3.3. However, this benefit is very limited when a_r varies from 4 to 2. The two respective curves achieve very similar performance as shown in Figure 5. This is because the noise can not be thoroughly eliminated even if more samples are selected from the same sample stream. It can also be observed that there is a gap between the RMSE of the proposed method and the CRB even in high SNR region. This is consistent with the conclusion in [35] where the authors claim that the RMSE of coprime configuration converges to a positive value and CRB tends to zero

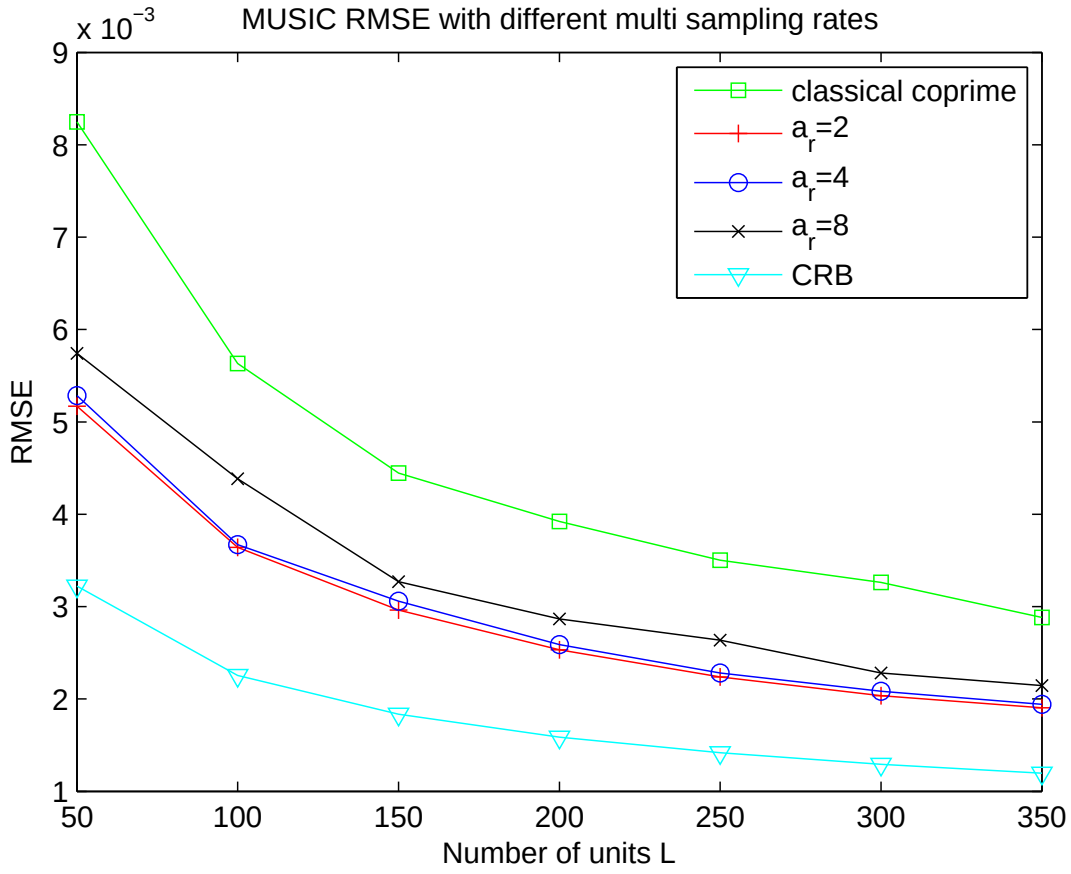

Figure 6: RMSE performance with different multi-rate coefficients, $M = 2, N = 3$, 4 sinusoidal components.

when $D < M + N$. Figure 6 compares the performance as a function of number of units. It is obvious that the estimation performance is improved when more sample units are available.

4.3. Comparison of data reusing and data no-reusing

Figure 7 and Figure 8 compare the data reusing mechanism and data no-reusing mechanism with the generalized coprime sampling scheme [26] and nuclear norm minimization interpolation scheme [27]. For the generalized coprime sampling scheme, we consider two sample units from each sampler to form a sample block hereafter. Different from the previous subsection with only one pair of holes, we consider $M = 4, N = 5$ such that six pairs of holes are required to be filled by choosing several different values of a_r simultaneously. The signal contains 12 sinusoidal components in Figure 7 and 25 components in Figure 8. As described in Section 4.1, three different multi-rate coefficients $\mathbb{I}_{rates} = \{2, 3, 29\}$ are considered to fill all the holes.

As shown in Figure 7 and Figure 8, both the data reusing and data no-reusing mechanism outperform

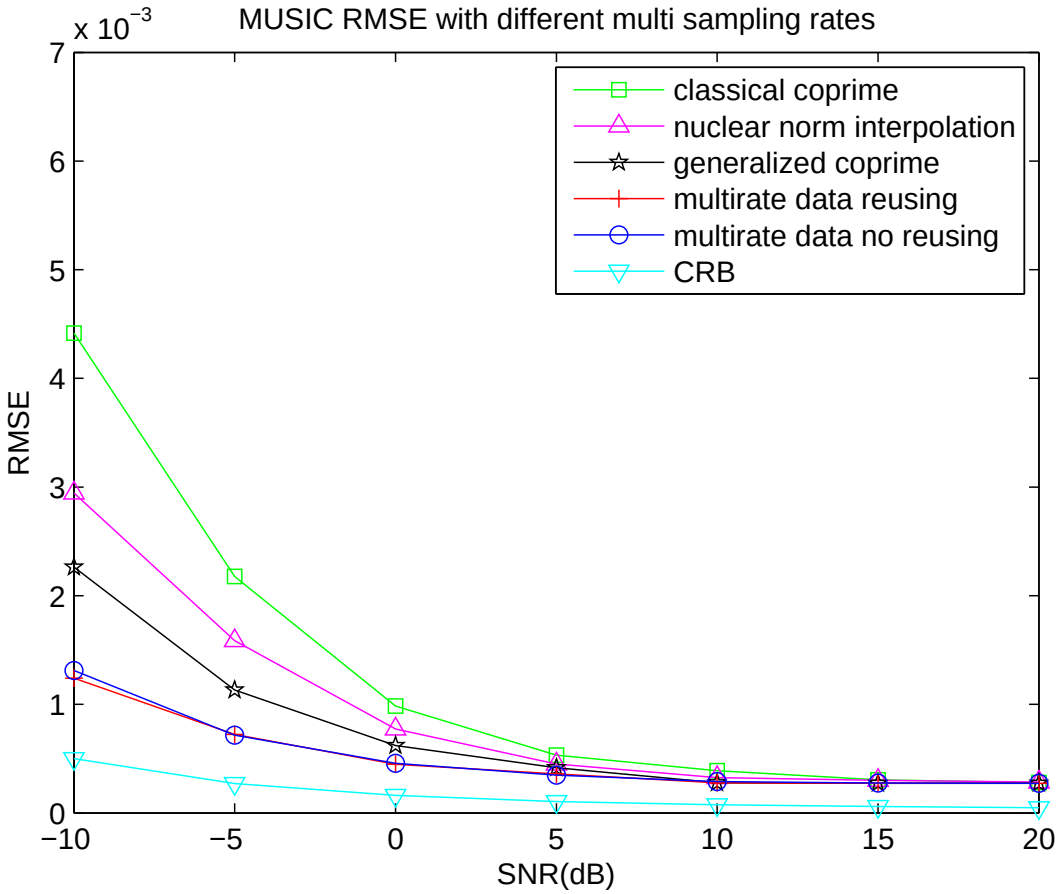

Figure 7: Performance of data reusing & data no-reusing, $M = 4, N = 5$, 12 sinusoidal components.

the generalized coprime and the nuclear norm scheme. This is because the generalized coprime scheme use two sample units to form a sample block in our simulation. By doing so, some holes can be filled but there still exist some unfilled holes and the maximum DOF can not be fully utilized. In contrast, the proposed method can fill all the holes distributed in $[0, (2M-1)N]$ and achieve better performance. In addition, the proposed method also surpasses the nuclear norm scheme because the performance of nuclear norm interpolation could be strongly affected by noise level. In high SNR region, nuclear norm scheme can achieve similar performance with the proposed method.

Furthermore, the data reusing mechanism has a slightly better performance than the data no-reusing mechanism when SNR is low because more data are employed for constructing the virtual coarray. As SNR increases, two mechanisms achieve very similar performance. This is because only part of data in $\hat{\mathbf{R}}_{\mathbf{y}}(a_r)$ is selected for the data reusing mechanism. The improvement will be very limited. It is evident in Figure

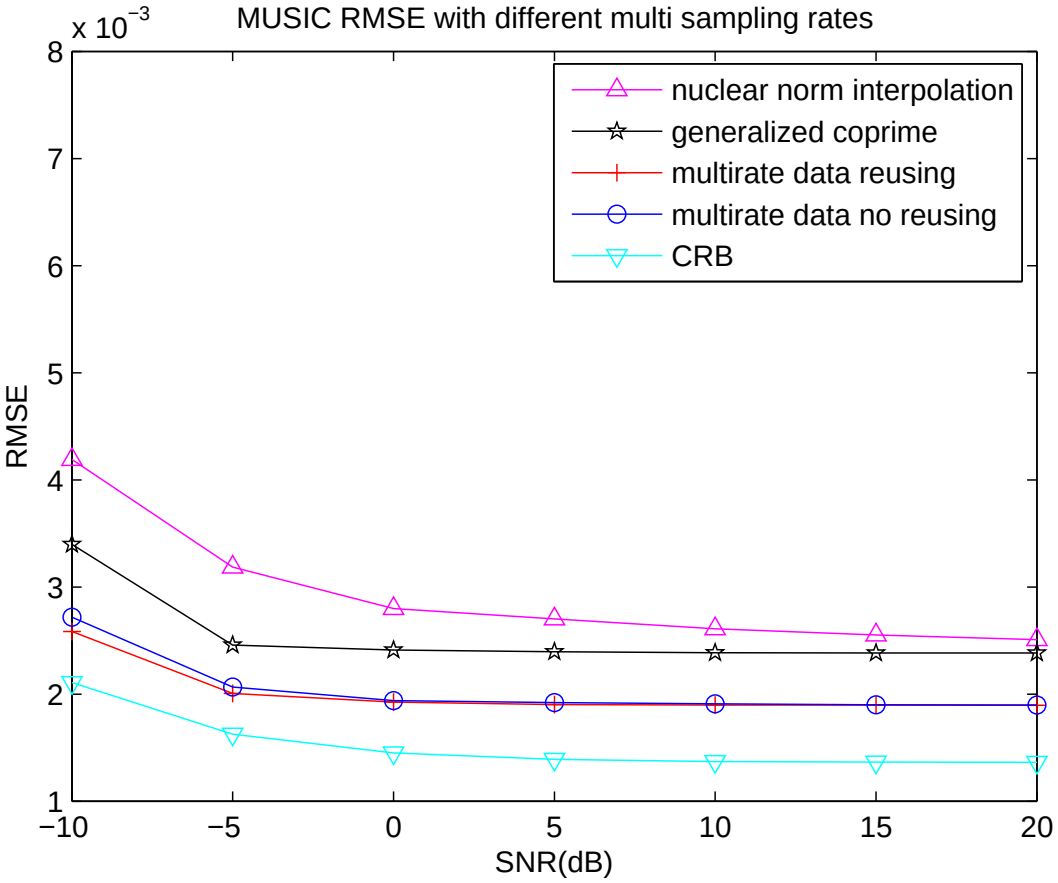

Figure 8: Performance of data reusing & data no-reusing, $M = 4, N = 5$, 25 sinusoidal components.

7 that in less sources scenario (i.e. 12 sinusoidal components compared to 25 components in Figure 8), the performance of the generalized coprime can be close to the proposed method when SNR is high. For $M = 4, N = 5$, the maximum number of detectable frequencies of the generalized coprime is 28, while it is 23 for the classical coprime and 35 for the proposed method. It should be mentioned that the nuclear norm scheme can not always achieve the maximum DOF because the actual freedom is governed by non-uniform grid [27]. We consider 25 sinusoidal components in Figure 8 for comparison. It can be seen that there is a gap between the generalized coprime and the proposed method due to the difference of DOF. The performance of nuclear norm scheme is the worst in Figure 8 and it tends to be close to the generalized coprime scheme in high SNR scheme. An interesting fact is that the virtual coarray of the generalized coprime scheme is similar to the classical coprime. The proposed method can also be easily applied to the generalized coprime scheme to fill the holes and the DOF can be further increased.

5. Conclusion

In this paper, we have proposed a multi-rate coprime sampling approach to fill the missing elements in the coprime virtual coarray without requiring additional samples. The maximum DOF can be exploited by fully utilizing the information contained in the classical coprime sampling. The proposed approach generates several scaled versions of the virtual coarray which are related to the multi-rate coefficients. The holes in the virtual coarray of the classical coprime sampling can be filled via selecting appropriate elements from the scaled virtual coarrays. The covariance matrix of the virtual coarray signal can be constructed after filling all the holes and more sources can be detected because the aperture of the coarray is increased. Furthermore, our proposed approach brings no extra sampling burden to the samplers. This is achieved by setting the multi-rate coefficient to a positive integer in accordance with the positions of the holes and part of the samples from the classical coprime sample stream can be directly selected to construct the multi-rate sampling sample stream. The proposed method can also be extended to the generalized coprime sampling to fill the holes and further increase the DOF. We also give the closed-form expression of holes in this paper to get a better choice of the multi-rate coefficients. The results reveal that our proposed scheme can achieve a higher number of detectable frequencies as well as better accuracy.

Acknowledgment

This work was supported in part by 2017-2019 Sino-French CAI Yuanpei Program, Guangzhou Science & Technology Program (No. 201807010071), NSFC (No. 61673260) and the China Scholarship Council (No. 201706150085).

6. Appendix

Proof of Proposition

1) The first hole is located at position $MN + M$ [26]. We first show that any integer number in $[0, MN + M - 1]$, namely a, can be generated by the difference coarray $\pm(Nm - Mn)$. We can rewrite $a = Nm - Mn$ into

$$Nm = a + Mn$$

Under the conditions $0 \leq n \leq N - 1$ and $0 \leq a \leq MN + M - 1$, for each value of a and n, we can have $a + Mn \leq 2MN - 1$. Then, it can be obtained that $N \leq Nm \leq 2MN - 1$, which is equivalent to

$1 \leq m \leq 2M - \frac{1}{N}$. As $N > 1$ and m is an integer, we can obtain

$$1 \leq m \leq 2M - 1$$

It indicates that for each value of $n \in [0, N-1]$, we can always find an appropriate value of $m \in [1, 2M-1]$ to obtain $a \in [0, MN + M - 1]$.

Then we show that the value $MN + M$ can not be obtained with $\pm(Nm - Mn)$ by using contradiction. Assuming that $MN + M = Nm - Mn$ can be obtained with some appropriate values of m, n. Then it can be derived that

$$\frac{M}{N} = \frac{m - M}{n + 1}$$

Notice that $m - M \leq M - 1$. But as M, N are coprime integers, their ratio can not be reduced to a radio of smaller integers. As a consequence, it is not possible to find proper values of m and n satisfying the above equation. Similar derivation holds if we assume $MN + M = -(Nm - Mn)$. Hence the first hole in position $MN + M$ is proved.

2) The general expression of positions of the holes $b_1 M + b_2 N$ $(b_1 \geq 1, b_2 \geq M)$ can be proved by contradiction, which can be found in Appendix I [34].

3) Finally, we determine the upper bounds of $b_1 and b_2$. Notice that the maximum number in $\mathbb{L}$ is $(2M-1)N$, the positions of the holes follow that $b_1 M + b_2 N < (2M-1)N$. Recalling the condition $b_1 \geq 1, b_2 \geq M$, we can have

$$\begin{aligned} b_1 M &< (2M-1)N - b_2 N \\ &< 2MN - N - MN \\ &< MN - N \\ b_1 &< N - \frac{N}{M} \end{aligned}$$

Since $N > M$ and b_1 is an integer, we can obtain that $b_1 \leq N - 1 - \lfloor \frac{N}{M} \rfloor$. Similarly, we can also obtain that $b_2 \leq 2M - 2$.

References

[1] J. Mitola, G. Q. Maguire, Cognitive radio: making software radios more personal, IEEE personal communications 6 (4) (1999) 13–18 (1999).

[2] E. Axell, G. Leus, E. G. Larsson, H. V. Poor, Spectrum sensing for cognitive radio: State-of-the-art and recent advances, IEEE Signal Process. Mag. 29 (3) (2012) 101–116 (2012).

[3] T. Yucek, H. Arslan, A survey of spectrum sensing algorithms for cognitive radio applications, IEEE communications surveys & tutorials 11 (1) (2009) 116–130 (2009).

[4] Y. Ma, Y. Gao, Y.-C. Liang, S. Cui, Reliable and efficient sub-nyquist wideband spectrum sensing in cooperative cognitive radio networks, IEEE Journal on Selected Areas in Communications 34 (10) (2016) 2750–2762 (2016).

[5] S. A. Razavi, M. Valkama, D. Cabric, Covariance-based OFDM spectrum sensing with sub-Nyquist samples, Signal Processing 109 (2015) 261–268 (2015).

[6] H. Sun, A. Nallanathan, C.-X. Wang, Y. Chen, Wideband spectrum sensing for cognitive radio networks: a survey, IEEE Wireless Communications 20 (2) (2013) 74–81 (2013).

[7] H. Sun, D. I. Laurenson, C.-X. Wang, Computationally tractable model of energy detection performance over slow fading channels, IEEE Communications Letters 14 (10) (2010) 924–926 (2010).

[8] D. Cabric, S. M. Mishra, R. W. Brodersen, Implementation issues in spectrum sensing for cognitive radios, in: Signals, systems and computers, 2004. Conference record of the thirty-eighth Asilomar conference on, Vol. 1, Ieee, 2004, pp. 772–776 (2004).

[9] J. Shi, W. Xiang, X. Liu, N. Zhang, A sampling theorem for the fractional Fourier transform without band-limiting constraints, Signal Processing 98 (2014) 158–165 (2014).

[10] J. Shi, X. Liu, L. He, M. Han, Q. Li, N. Zhang, Sampling and reconstruction in arbitrary measurement and approximation spaces associated with linear canonical transform, IEEE Transactions on Signal Processing 64 (24) (2016) 6379–6391 (2016).

[11] J. Shi, X. Liu, X. Sha, Q. Zhang, N. Zhang, A sampling theorem for fractional wavelet transform with error estimates, IEEE Transactions on Signal Processing 65 (18) (2017) 4797–4811 (2017).

[12] M. Mishali, Y. C. Eldar, From theory to practice: Sub-Nyquist sampling of sparse wideband analog signals, IEEE Journal of Selected Topics in Signal Processing 4 (2) (2010) 375–391 (2010).

[13] D. Cohen, Y. C. Eldar, Sub-Nyquist cyclostationary detection for cognitive radio, IEEE Transactions on Signal Processing 65 (11) (2017) 3004–3019 (2017).

[14] N. Fu, G. Huang, L. Zheng, X. Wang, Sub-Nyquist sampling of multiple sinusoids, IEEE Signal Processing Letters (2018).

[15] J. Chen, Q. Liang, B. Zhang, X. Wu, Spectrum efficiency of nested sparse sampling and coprime sampling, EURASIP Journal on Wireless Communications and Networking 2013 (1) (2013) 47 (2013).

[16] Y. Zhao, Y. H. Hu, J. Liu, Random triggering-based sub-Nyquist sampling system for sparse multiband signal, IEEE Transactions on Instrumentation and Measurement 66 (7) (2017) 1789–1797 (2017).

[17] S. Huang, H. Zhang, H. Sun, L. Yu, L. Chen, Frequency estimation of multiple sinusoids with three sub-Nyquist channels, Signal Processing 139 (2017) 96–101 (2017).

[18] R. T. Hoctor, S. A. Kassam, The unifying role of the coarray in aperture synthesis for coherent and incoherent imaging, Proceedings of the IEEE 78 (4) (1990) 735–752 (1990).

[19] P. Pal, P. Vaidyanathan, Nested arrays: A novel approach to array processing with enhanced degrees of freedom, IEEE Transactions on Signal Processing 58 (8) (2010) 4167–4181 (2010).

[20] H. Qiao, P. Pal, Generalized nested sampling for compression and exact recovery of symmetric Toeplitz matrices, in: 2014 IEEE Global Conference on Signal and Information Processing (GlobalSIP), IEEE, 2014, pp. 443–447 (2014).

[21] A. Moffet, Minimum-redundancy linear arrays, IEEE Transactions on antennas and propagation 16 (2) (1968) 172–175 (1968).

[22] M. Ishiguro, Minimum redundancy linear arrays for a large number of antennas, Radio Science 15 (6) (1980) 1163–1170 (1980).

[23] P. P. Vaidyanathan, P. Pal, Sparse sensing with co-prime samplers and arrays, IEEE Transactions on Signal Processing 59 (2) (2011) 573–586 (2011).

[24] P. Pal, P. P. Vaidyanathan, Coprime sampling and the MUSIC algorithm, in: Digital Signal Processing Workshop and IEEE Signal Processing Education Workshop (DSP/SPE), 2011 IEEE, IEEE, 2011, pp. 289–294 (2011).

[25] Z. Fu, P. Chargé, Y. Wang, Coprime sampling with embedded random delays, Signal Processing 158 (2019) 150–155 (2019).

[26] S. Qin, Y. D. Zhang, M. G. Amin, A. M. Zoubir, Generalized coprime sampling of Toeplitz matrices for spectrum estimation, IEEE Transactions on Signal Processing 65 (1) (2017) 81–94 (2017).

[27] C.-L. Liu, P. Vaidyanathan, P. Pal, Coprime coarray interpolation for DOA estimation via nuclear norm minimization, in: Circuits and Systems (ISCAS), 2016 IEEE International Symposium on, IEEE, 2016, pp. 2639–2642 (2016).

[28] H. Qiao, P. Pal, Gridless line spectrum estimation and low-rank Toeplitz matrix compression using structured samplers: A regularization-free approach, IEEE Transactions on Signal Processing 65 (9) (2017) 2221–2236 (2017).

[29] X. Wu, W.-P. Zhu, J. Yan, A Toeplitz covariance matrix reconstruction approach for direction-of-arrival estimation, IEEE Transactions on Vehicular Technology 66 (9) (2017) 8223–8237 (2017).

[30] M. Guo, T. Chen, B. Wang, An improved DOA estimation approach using coarray interpolation and matrix denoising, Sensors 17 (5) (2017) 1140 (2017).

[31] C. Zhou, Y. Gu, X. Fan, Z. Shi, G. Mao, Y. D. Zhang, Direction-of-arrival estimation for coprime array via virtual array interpolation, IEEE Transactions on Signal Processing (2018).

[32] E. BouDaher, Y. Jia, F. Ahmad, M. G. Amin, Multi-frequency co-prime arrays for high-resolution direction-of-arrival estimation., IEEE Trans. Signal Processing 63 (14) (2015) 3797–3808 (2015).

[33] J. L. Moulton, Enhanced high-resolution imaging through multiple-frequency coarray augmentation, Ph.D. thesis, University of Pennsylvania (2010).

[34] S. Qin, Y. D. Zhang, M. G. Amin, Generalized coprime array configurations for direction-of-arrival estimation, IEEE Transactions on Signal Processing 63 (6) (2015) 1377–1390 (2015).

[35] M. Wang, A. Nehorai, Coarrays, MUSIC, and the Cramér–Rao bound, IEEE Transactions on Signal Processing 65 (4) (2017) 933–946 (2017).

[36] R. Schmidt, Multiple emitter location and signal parameter estimation, IEEE transactions on antennas and propagation 34 (3) (1986) 276–280 (1986).

[37] R. Roy, T. Kailath, ESPRIT-estimation of signal parameters via rotational invariance techniques, IEEE Transactions on acoustics, speech, and signal processing 37 (7) (1989) 984–995 (1989).

[38] P. Stoica, A. Nehorai, MUSIC, maximum likelihood, and Cramer-Rao bound, IEEE Transactions on Acoustics, Speech, and Signal Processing 37 (5) (1989) 720–741 (1989).

[39] P. Stoica, A. Nehorai, Performance study of conditional and unconditional direction-of-arrival estimation, IEEE Transactions on Acoustics, Speech, and Signal Processing 38 (10) (1990) 1783–1795 (1990).

[40] C.-L. Liu, P. Vaidyanathan, Cramér–Rao bounds for coprime and other sparse arrays, which find more sources than

sensors, Digital Signal Processing 61 (2017) 43–61 (2017).

[41] A. Koochakzadeh, P. Pal, Cramér–Rao bounds for underdetermined source localization, IEEE Signal Processing Letters 23 (7) (2016) 919–923 (2016).